
Immunoscintigraphy of Aortic Dissection with ^{99m}Tc -Labeled Murine Anti-Smooth Muscle Myosin Monoclonal Antibody in Rats

Toshiya Iwasaki, Tsutomu Iwasaki, Yasushi Aihara, Tsugiyasu Kanda, Noboru Oriuchi, Keigo Endo, Hirohisa Katoh, Toru Suzuki, and Ryozo Nagai

Second Department of Internal Medicine and Department of Nuclear Medicine, Gunma University School of Medicine, Gunma; Immunology Laboratory, Diagnostic Division, Yamasa Corporation, Chiba; and Department of Cardiovascular Medicine, University of Tokyo Graduate School of Medicine, Tokyo, Japan

Aortic dissection is among the most common of fatal conditions of the aorta. Prompt and accurate diagnosis of the site and extent of the lesion is necessary for adequate therapy. However, this catastrophic disease, characterized by extensive damage to smooth muscle cells, lacks specific signs and symptoms. As a result, the diagnosis is still frequently missed today and a new diagnostic method to specifically identify aortic dissection would be attractive. The purpose of this study was to examine the feasibility of radioimmunoscintigraphy using ^{99m}Tc -anti-smooth muscle myosin monoclonal antibody (SM-MAb) for the noninvasive diagnosis of aortic dissection in the rat experimental model. **Methods:** The accumulation of ^{99m}Tc -anti-SM-MAb was studied, and scintigraphic imaging with ^{99m}Tc -anti-SM-MAb was performed in rats immediately after experimental aortic dissection and 1 and 2 wk later. **Results:** The radioactivity of ^{99m}Tc -anti-SM-MAb in the dissected aorta showed a significant increase compared both with the normal portion of the aorta and with blood 6 h after injection of the radiotracer; the ratio of the percentage injected dose per gram (%ID/g) in the lesion to that retained in the normal portion was 4.17 ± 1.47 . Scintigraphic imaging with ^{99m}Tc -anti-SM-MAb allowed distinct visualization of the dissected aorta with specific accumulation of antibody 6 h after tracer injection. Selective accumulation of the tracer in the dissected portion of the aorta persisted even 1 wk after aortic injury, allowing clear visualization of the dissected lesion by scintigraphy. **Conclusion:** Radioimmunoscintigraphy using anti-SM-MAb is a potentially useful noninvasive diagnostic method for imaging aortic dissection.

Key Words: radioimmunoscintigraphy; myosin; smooth muscle; dissecting aortic aneurysm

J Nucl Med 2001; 42:130–137

Aortic dissection is a common fatal condition of the aorta and carries a mortality rate as high as 50% if left untreated during the first 48 h after onset of symptoms (1,2).

Received Mar. 10, 2000; revision accepted Jul. 31, 2000.

For correspondence or reprints contact: Ryozo Nagai, MD, Department of Cardiovascular Medicine, University of Tokyo Graduate School of Medicine, 3-7-1 Hongo, Bunkyo, Tokyo, 113-0033 Japan.

Adequate therapy requires accurate diagnosis regarding the site and extent of dissection. Over the past 25 y, great strides have been made in clinical diagnostic methods. In particular, new imaging techniques such as MRI, CT, transesophageal and transthoracic echocardiography, and angiography have greatly improved the accuracy of the diagnosis of aortic dissection (3). However, these methods detect only morphologic alterations, lacking specificity for the disease. Moreover, because patients with aortic dissection may be hemodynamically and generally unstable, invasive diagnostic procedures or imaging using contrast medium may be difficult to perform; thus, a timely diagnosis can be missed. A disease-specific, noninvasive imaging method applicable to aortic dissection would be attractive.

Aortic dissection is characterized by extensive damage to smooth muscle cells, leading to release of intracellular structural proteins, including smooth muscle myosin heavy chain (SM-MHC), into the circulation. Recently, a novel biochemical method developed to diagnose aortic dissection by immunoassay of serum SM-MHC using a specific anti-SM-MHC monoclonal antibody (MAb) (4,5) has shown promise as a sensitive marker for aortic dissection (6).

Recent advances in radioimmunoscintigraphy using markers specific for various diseases have been reported as well. For example, radioimmunoscintigraphy using anticardiac myosin MAb has been developed as a useful diagnostic imaging method for myocardial infarction or acute myocarditis (7–9). Radioimmunoscintigraphy of vascular atherosclerotic lesions using monoclonal or polyclonal antibodies has also been reported (10,11). However, radioimmunoscintigraphy of aortic dissection using a MAb to detect aortic smooth muscle cell damage has not been available. Our objective was to examine the feasibility of radioimmunoscintigraphy using a smooth muscle-specific MAb for noninvasive diagnosis of aortic dissection. In this study, we used a biodistribution study and gamma scintigraphy to investigate the accumulation of ^{99m}Tc -labeled smooth muscle-specific antibodies in rats with experimental aortic dissection.

MATERIALS AND METHODS

Preparation of MAb and Cross-Reactivity to Rat Smooth Muscle Myosin

Anti-smooth muscle myosin MAb (SM-MAb) was produced by conventional hybridoma methods, immunizing mice with purified human uterine smooth muscle myosin as described previously (5). This anti-SM-MAb recognized the tail portion of SM-MHC, and we could detect smooth muscle myosin at the level of 0.1 ng/mL (2 pmol/L) by double monoclonal sandwich enzyme immunoassay using this MAb (5). To determine specific cross-reactivity with rat smooth muscle myosin, immunohistochemical studies were performed on rat aorta. Specimens obtained from a normal male Wistar rat (Institute of Experimental Animal Research, Gunma University School of Medicine) were fixed with 95% ethanol, dehydrated, and embedded in paraffin. Sections were cut from tissue blocks at a thickness of 16 μ m, dewaxed, and rehydrated. Immunohistochemical staining was performed as previously described (12), using anti-chloramphenicol acetyltransferase (CAT) MAb to exclude nonspecific reactivity.

Radiolabeling of Anti-SM-MAB

^{99m}Tc labeling of the MAb was performed according to a method previously reported (13,14). Monoclonal antibodies (2 mg/mL in citrate-buffered saline, 0.1 mol/L, pH 6.0) were reduced by 0.94 μ L 2-mercaptoethanol (Sigma Chemical, St. Louis, MO) at a 2-mercaptoethanol-to-MAb molar ratio of 1000:1 at room temperature for 30 min. The reduced antibodies then were purified by PD-10 column chromatography. The protein fraction was kept frozen in 0.3-mL aliquots containing 0.2 mg antibody at -80°C . Immediately before antibody administration to rats, 0.2 mg reduced antibody was thawed. Stannous chloride (2.5 μ g) was dissolved in 50 μ L hydrochloric acid saline solution (0.06 N), which then was mixed with the antibody. The mixture was incubated for 60 min at room temperature with 740 MBq ^{99m}Tc -pertechnetate eluted from a ^{99}Mo - ^{99m}Tc generator (Ultra-Techne Kow; Daiichi Radioisotope Laboratories, Tokyo, Japan). Instant thin-layer paper chromatography (ITLC-SG; German Sciences, Ann Arbor, MI) was performed with acetone as the eluent before injection. More than 98% of radioactivity remained protein bound at all times.

Animals and Surgery

The animal studies were performed in accordance with the policy statement "Position of the American Heart Association on Research Animal Use." Seventy male Wistar rats weighing 300 g were anesthetized by intraperitoneal administration of sodium pentobarbital (40 mg/kg). Ten of these rats underwent a sham operation (Fig. 1). After midline abdominal and femoral incision, the aorta and femoral artery were exposed, and a spring-coil guidewire was advanced into the abdominal aorta through a cannula inserted into the femoral artery. The guidewire was withdrawn three times during extraaortic compression with the forceps in three directions to produce abdominal aortic dissection. After intra-arterial injection of heparin (100 IU/kg), the femoral artery was ligated and the incisions were sutured. The rats were distributed into 14 groups of five animals each. Six groups received tracer antibody injections immediately after surgery. The remaining 8 groups recovered from anesthesia and were housed in individual cages for 1 or 2 wk until tracer antibody administration. Seventy-four megabecquerels ^{99m}Tc -anti-SM-MAB (containing approximately 20 μ g antibody) were injected into 8 groups of rats (2 groups of sham-operated rats,

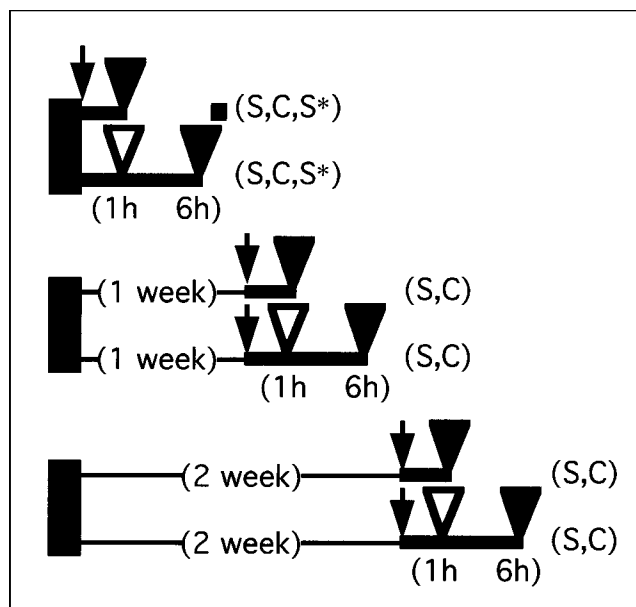


FIGURE 1. Experimental protocol. Rectangles = surgical procedure; arrows = injection of radiotracer; S = group of five rats with aortic dissection who received ^{99m}Tc -anti-SM-MAB injections; C = group of five rats with aortic dissection who received ^{99m}Tc -anti-CAT-MAB injections; S* = group of five rats with sham operation who received ^{99m}Tc -anti-SM-MAB injections; open arrowheads = scintigraphic imaging; closed arrowheads = scintigraphic imaging including ex vivo scintigraphy and biodistribution assessment including autoradiography.

2 groups studied immediately after the procedure, 2 groups studied after 1 wk, and 2 groups studied after 2 wk). In 6 other groups, 74 MBq ^{99m}Tc -labeled anti-CAT-MAB were injected (2 groups studied immediately after the procedure, 2 groups studied after 1 wk, and 2 groups studied after 2 wk). Radiolabeled antibodies were injected through the femoral vein under light anesthesia with pentobarbital. Rats that underwent sham operation received ^{99m}Tc -anti-SM-MAB injections only immediately after the aortic injury. Rats injected with ^{99m}Tc -anti-CAT-MAB were used as negative controls.

^{99m}Tc -Anti-SM-MAB Imaging

Radioimmunoscintigraphy was performed 1 h after injection of the radiotracer in all 14 groups and was repeated 6 h after injection in 7 groups, with the rats under light anesthesia with pentobarbital. Additional anesthetic was administered when required. Whole-body planar images were obtained in the anterior views with a gamma camera (GCA-901A/HG; Toshiba, Tokyo, Japan) equipped with a low-energy, parallel-hole, high-resolution collimator and stored on a 512×512 pixel matrix by means of a digital computer (GMS-5500; Toshiba). Images were recorded for a preset time of 10 min at the energy peak of 140 keV with a 20% window. Immediately after completion of planar imaging, pinhole SPECT images were acquired using a rotating gamma camera equipped with a tungsten pinhole insert with 2.0-mm-diameter apertures in a low-energy pinhole collimator in a 64×64 pixel matrix, with a zoom factor of 2. This imaging procedure was performed as previously described (15), with minor modifications. Projection data were collected in 6° increments over 360° in the step-and-shoot mode using a 30-mm radius of rotation. In planar images, the regional count within the region of interest set on the

dissected aorta was divided by the count in a region of interest set on the superior mediastinal area to yield a ^{99m}Tc -labeled antibody uptake ratio. All scintigrams were interpreted by two observers unaware of the specific experimental conditions for the individual animals evaluated.

Ex Vivo Scintigraphy and Biodistribution Study

Immediately after the last scintigraphic acquisition, 200 μL blood were aspirated through the femoral vein with the animals under pentobarbital anesthesia, and the same volume of urine was aspirated by bladder puncture. After the rats were killed with an overdose of pentobarbital, they were bled. The affected aortas were removed and mounted on a gamma camera equipped with a low-energy, parallel-hole, high-resolution collimator for 10 min for ex vivo scintigraphy. After the acquisition, the following organs and tissues were removed, weighed, and counted in a well scintillation gamma counter: aorta (normal and injured portions), heart, lung, liver, spleen, kidney, stomach, muscle, and bone. The radioactivity of 200 μL blood and urine also was counted. Radioactivity uptake in tissues was expressed as percentage injected dose per gram of tissue (%ID/g).

Autoradiography

After completion of sampling for the biodistribution study, dissected aortas were frozen at -80°C in liquid nitrogen. Sections were cut at 16- μm thickness at -30°C using a cryostat. Sections were placed on clean glass slides and air dried for 10 min. The glass slides were mounted on cardboard and apposed to radiographic film for 12 h of exposure.

Histopathologic Examination

After autoradiographic processing, the sections on the slides were stained with hematoxylin and eosin for light microscopic examination. Immediately before ex vivo scintigraphy, small tissue blocks were obtained from the injured portion of the aorta in one rat from each group. These blocks were fixed in 3% phosphate-buffered glutaraldehyde solution (pH 7.4) for 3 h at 4°C and processed for electron microscopy by routine methods.

Statistical Analysis

Data are expressed as the mean value \pm SD, and statistical analysis was performed using one-way ANOVA and the Student *t* test. Differences associated with a value of $P < 0.05$ were accepted as statistically significant.

RESULTS

Anti-SM-MAb Immunostaining

Immunohistochemical staining of sections of rat aorta showed the specific reactivity of anti-SM-MAb in the smooth muscle cell layer (Fig. 2A). Anti-CAT-MAb showed no staining (Fig. 2B).

Experimental Aortic Dissection

Immediately after the dissection injury, the aortic intima was almost completely disrupted. Many foci of medial tearing with irregular discontinuities and disorganization of the inner musculoelastic layer also were noted. However, no massive blood clotting or macrophage infiltration was noted. These findings were most prominent immediately after the experimental dissection but were frequently still seen 1 wk after dissection. Two weeks after dissection, the

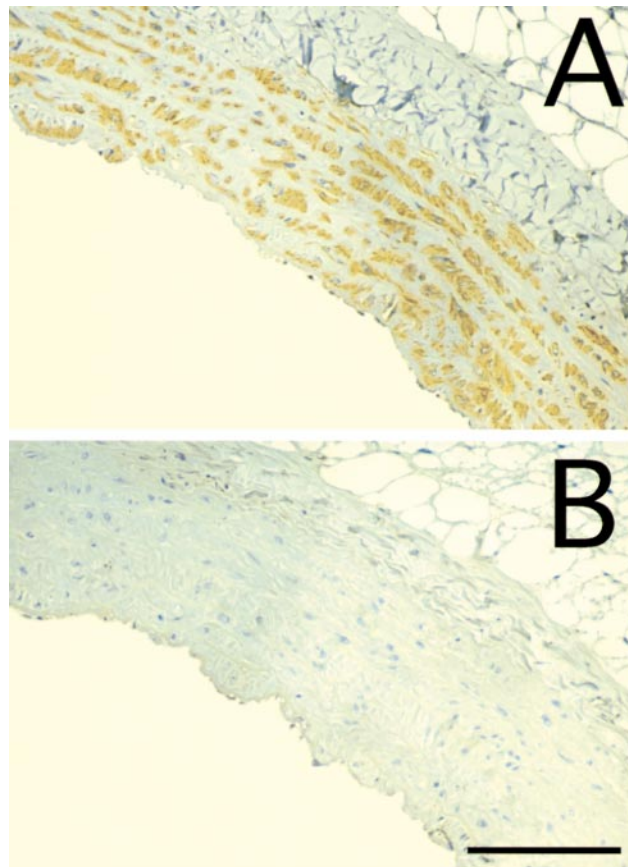


FIGURE 2. Immunohistochemical staining of rat aorta. Transverse sections of abdominal aorta are stained with anti-SM-MAb (A) and anti-CAT-MAb (B). Scale bar = 0.1 mm.

injured wall was nearly repaired, showing reendothelialization and medial thickening consisting of smooth muscle cell proliferation. In the interstitial space, fibroblasts, fibrocytes, macrophages, and lymphocytes were frequently observed at 1 and 2 wk after injury, but form cells were scarcely noted. Electron microscopically, newly dissected lesions frequently showed dead or dying smooth muscle cells with disruption of cell membranes, nuclear pyknosis, mitochondrial swelling, and dilation of endoplasmic reticulum, as reported previously (16).

^{99m}Tc -Anti-SM-MAb Imaging

Representative planar images of rats with aortic dissection at 6 h after injection are shown in Figure 3. In the initial images for each tracer, at 1 h postinjection, visceral blood-pool activities predominated, obscuring specific accumulation of ^{99m}Tc -anti-SM-MAb in the lesion. Radioactivity was redistributed specifically to the aortic lesion 6 h after injection. The lesion was readily recognized as a discrete area of ^{99m}Tc -anti-SM-MAb immediately after the procedure (Fig. 3A). One week after aortic injury, the dissected aorta could still be recognized (Fig. 3B), whereas 2 wk after injury, the dissected lesion no longer was clearly visualized (Fig. 3C).

To quantitatively determine specific accumulation, we used uptake ratios of ^{99m}Tc -labeled monoclonal antibodies.

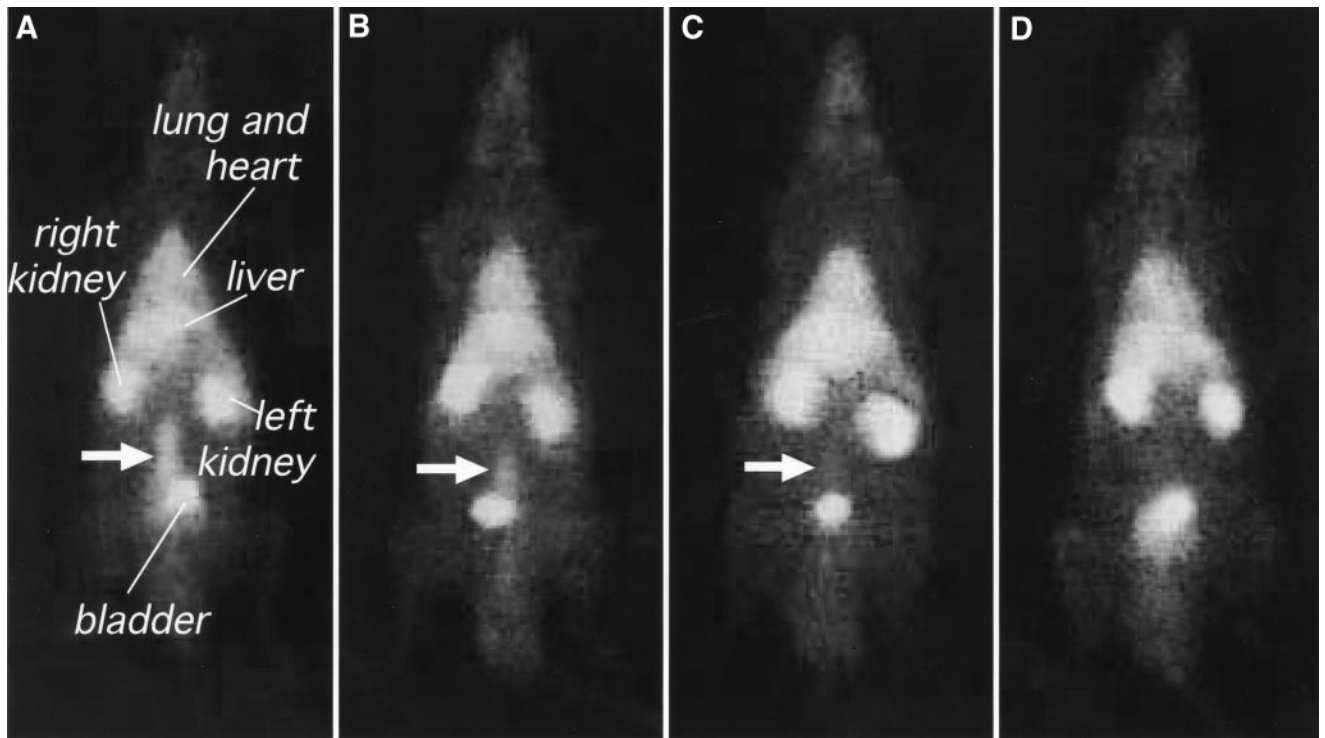


FIGURE 3. Immunoscintigrams with ^{99m}Tc -SM-MAB (A–C) and ^{99m}Tc -anti-CAT-MAB (D) 6 h after injection of tracer are anterior whole-body images of rats with aortic dissection (immediately after dissection [A and D]; 1 wk after dissection [B]; and 2 wk after dissection [C]). Selective accumulation (arrows) of ^{99m}Tc -anti-SM-MAB in dissected aorta was clearly observed immediately and 1 wk after dissection and became less intense at 2 wk, so that lesion could no longer be detected (C). No accumulation of ^{99m}Tc -anti-CAT-MAB was seen in lesion (D).

The ^{99m}Tc -labeled anti-SM-MAB uptake ratio for the dissected aorta was significantly greater 6 h after injection than the ratio for ^{99m}Tc -anti-CAT-MAB, except for images obtained 2 wk after the injury (Fig. 4). Nonspecific radioactivity was observed in the lung, heart, liver, kidney, and bladder of all rats, representing blood-pool activity and excretion of ^{99m}Tc -MAB.

In SPECT images, accumulation of ^{99m}Tc -anti-SM-MAB in the dissected aorta could be observed more distinctly, and stereologic localization of the lesion was precise and unambiguous (Fig. 5A). As in the planar image, the dissected lesion in SPECT could be recognized at 1 wk after experimental dissection (Fig. 5B) but not at 2 wk (Fig. 5C). No obvious radioactivity of ^{99m}Tc -anti-CAT-MAB could be seen in lesions during the study either in planar images (Fig. 3D) or in SPECT images (Fig. 5D). Scintigraphic images of rats that underwent sham operations did not show notable accumulations of tracer in the aortic lesion.

Biodistribution of ^{99m}Tc -Labeled Anti-SM-MAB

The results of the biodistribution study are summarized in Figure 6. The %ID/g of normal tissues (with the exception of the kidneys and urine) was generally decreased during the study as the tracer was cleared from the circulation. Distribution levels of most of the normal tissue at 1 h after injection of the tracer dropped to approximately one half after 6 h. Impressively, the biodistribution in the dissected

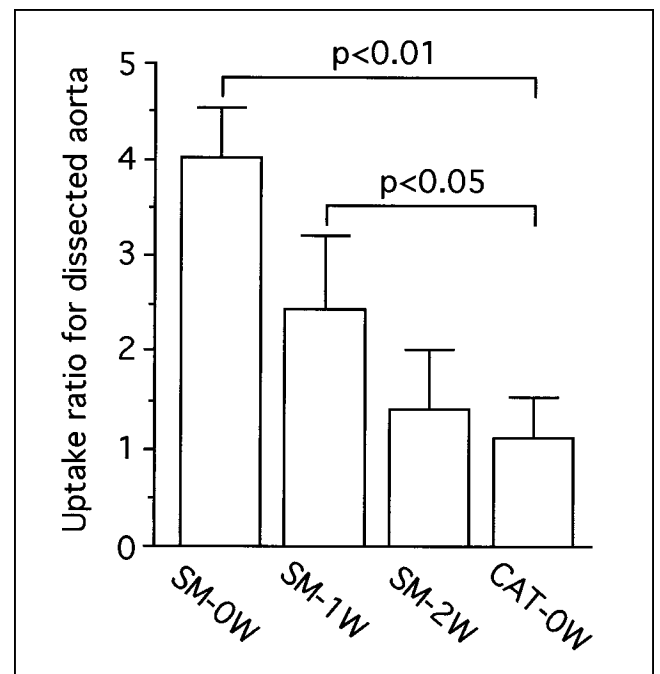


FIGURE 4. Uptake ratios of ^{99m}Tc -anti-SM-MAB (SM-0W, SM-1W, and SM-2W) and ^{99m}Tc -anti-CAT-MAB (CAT-0W) in dissected aorta 6 h after tracer injection. SM-0W and CAT-0W = dissected portion of aorta immediately after dissection; SM-1W = dissected portion of aorta 1 wk after dissection; SM-2W = dissected portion of aorta 2 wk after dissection. Data are expressed as mean \pm SD.

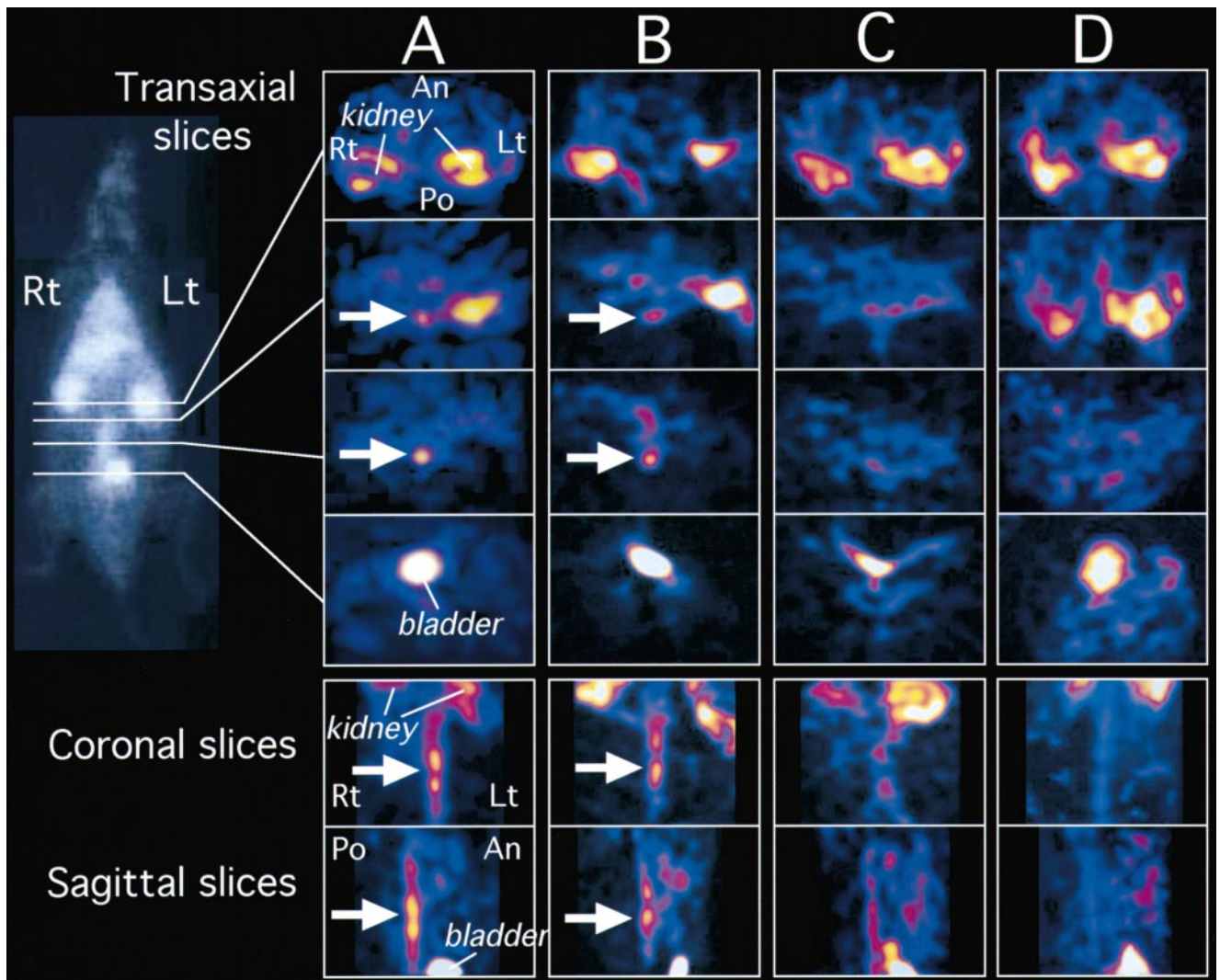


FIGURE 5. Transaxial, coronal, and sagittal immunoscintigraphy SPECT images, corresponding to planar images in Figure 3, of rats with aortic dissection. Horizontal lines in planar image (left) show areas through which transaxial sections were reconstructed. Immediately and 1 wk after dissection, prominent selective accumulation of ^{99m}Tc -anti-SM-MAB in dissected aorta was easily recognized (arrows). Two weeks after procedure, dissected lesion could not be clearly visualized (C) and was similar to appearance in rat with ^{99m}Tc -anti-CAT-MAB (D). An = anterior; Lt = left; Po = posterior; Rt = right.

aorta contrasted with the other tissues immediately after the dissection. Sustained accumulation of ^{99m}Tc -anti-SM-MAB after an initially high level at 1 h was observed in the dissected lesion of the aorta at 6 h. These results revealed that specific localization of ^{99m}Tc -anti-SM-MAB to the dissected lesion of the aorta at 6 h (15.12 ± 3.17 %ID/g) was significantly higher ($P < 0.01$) than was localization to the normal portion (3.62 ± 0.62 %ID/g) and to the blood (3.98 ± 1.97 %ID/g) (Fig. 6A). The ratio of ^{99m}Tc -anti-SM-MAB in the dissected aorta versus the normal portion immediately after the injury was significantly higher at 6 h after injection (4.17 ± 1.47 %ID/g) than at 1 h (1.79 ± 0.83 %ID/g). After 1 wk, the biodistribution of the dissected aorta showed similar results, with relatively low levels in the newly dissected lesion (Fig. 6B). After 2 wk, the levels were the same as those in the normal portion (Fig. 6C).

To exclude nonspecific accumulation of anti-SM-MAB to the lesion, the biodistribution of ^{99m}Tc -anti-CAT-MAB was studied. The accumulation of radiolabeled anti-CAT antibody in the dissected aorta did not show a significant difference from the normal portion during the experiment (Fig. 6D). The biodistribution studies of the sham-operated rats showed results similar to those for ^{99m}Tc -anti-CAT-MAB.

Ex Vivo Scintigraphy of the Dissected Aorta

Ex vivo scintigrams of aorta at 6 h after injection immediately after the injury showed a considerable specific accumulation of ^{99m}Tc -labeled anti-SM-MAB in the dissected region of the aorta (Fig. 7A). Ex vivo scintigrams for ^{99m}Tc -anti-CAT-MAB (Fig. 7B) and sham operations showed no accumulation throughout the experiment.

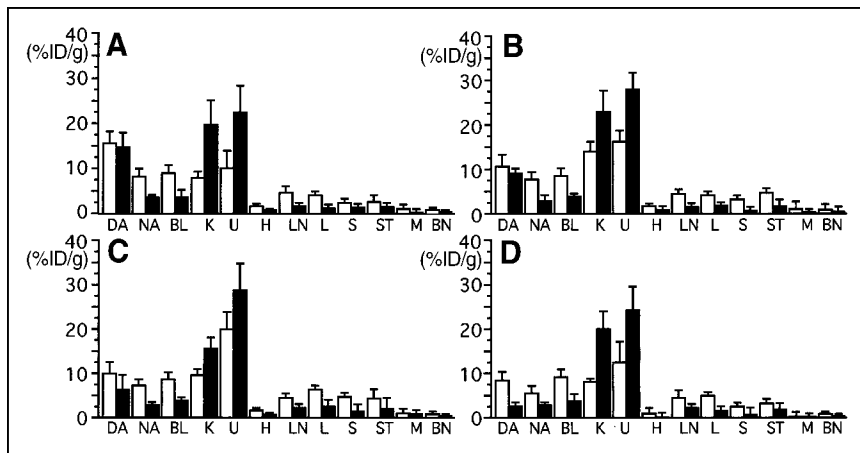


FIGURE 6. Biodistribution of ^{99m}Tc -anti-SM-MAb (A–C) and ^{99m}Tc -anti-CAT-MAb (D) in rats with experimental aortic dissection (immediately after dissection [A and D]; 1 wk after dissection [B]; and 2 wk after dissection [C]). White bar = %ID/g 1 h after injection of tracer; black bar = %ID/g 6 h after injection of tracer. Data are expressed as mean \pm SD. BL = blood; BN = bone; DA = dissected portion of aorta; H = heart; K = kidney; L = liver; LN = lung; M = muscle; NA = normal portion of aorta; S = spleen; ST = stomach; U = urine.

Autoradiography of the Dissected Aorta

Because the aortic wall of the rat is thin relative to the spatial resolution of the gamma camera used in this study, detailed imaging of the aortic wall could not be performed. Therefore, we performed autoradiography of the dissected aorta after ex vivo scintigraphy. Considerable accumulation of ^{99m}Tc -anti-SM-MAb in the dissected aortic wall (Fig. 7C), corresponding to the area of accumulation in the gamma images of Figure 7, was clearly shown by autoradiography. No specific accumulation was seen in the ^{99m}Tc -anti-CAT-MAb autoradiographs (Fig. 7D).

DISCUSSION

Radioimmunoimaging of vascular atherosclerotic lesions using monoclonal or polyclonal antibodies has been studied clinically and experimentally (10,11). However, immunoscintigraphy of aortic dissection using radiolabeled MAb has not been developed, primarily because of a lack of

markers specific for smooth muscle cells. Polyclonal human immunoglobulin G has been shown to localize to form cells in atherosclerotic lesions in a rabbit aortic denudation model 4–5 wk after injury (10). These form cells are largely macrophage derived and bear abundant Fc receptors. However, in this study the dissected lesions showed few form cells at 1 and 2 wk. Therefore, the accumulation of the tracer to Fc receptors on macrophage-derived form cells was not considered to play an important role in the radioimmunoimaging of this study. Indeed, ^{99m}Tc -anti-SM-MAb accumulated most intensely in dissected lesions immediately after aortic injury, before any atherosclerotic changes. Therefore, accumulation of the tracer that we used appeared to represent specific binding to myosin in damaged smooth muscle cells in the lesion.

In the dissected aorta, irreversible mechanical tissue injury results in a loss of cell membrane integrity, as evidenced by leakage of intracellular structural proteins, such

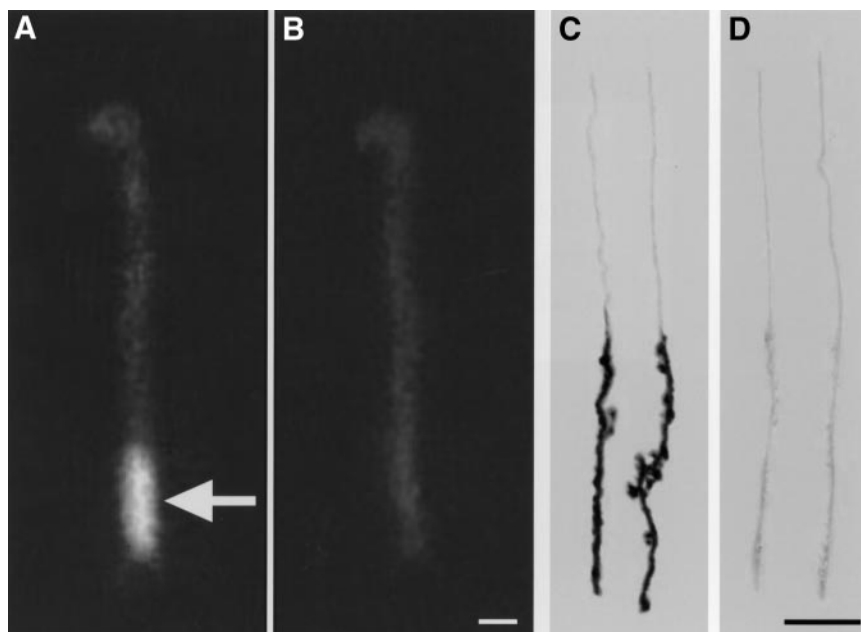


FIGURE 7. (A and B) Ex vivo radioimmunoscintigrams of aorta, including dissected lesions, in rats 6 h after injection of ^{99m}Tc -anti-SM-MAb (A) and ^{99m}Tc -anti-CAT-MAb (B). Tracers were injected immediately after dissection injury. Considerable specific accumulation of ^{99m}Tc -anti-SM-MAb was observed in lesion (arrow), but no accumulation of ^{99m}Tc -anti-CAT-MAb was seen (B). (C and D) Autoradiographs of same dissected aortas in ex vivo radioimmunoscintigrams. Distinct radioactivity of ^{99m}Tc -anti-SM-MAb was observed in dissected aortic wall (C), but no specific radioactivity of ^{99m}Tc -anti-CAT-MAb could be seen (D). Scale bar = 5 mm.

as myosin heavy chain, into the circulation (4–6). If the extracellular tracer is an antibody specific for an intracellular component, the proteins should enter the damaged cells and bind specifically to intracellular antigen. In patients with aortic dissection, exposed smooth muscle myosin provides a distinct target for an injected antimyosin antibody. Therefore, radiolabeled anti-SM-MAB specific for smooth muscle myosin could be used for immunoscintigraphic imaging of dissecting aortic aneurysm.

In the biodistribution study, anti-CAT-MAB showed a weak accumulation within the dissected lesion of the aorta 1 h after injection, but accumulation in the lesion was lower than for anti-SM-MAB, and anti-CAT-MAB also showed a decrease at 6 h to levels similar to those in the normal portion of aorta (Fig. 6D). These results indicate that the weak accumulation of anti-CAT-MAB in the dissected region during early phases of injury represented nonspecific entry of anti-CAT-MAB into damaged smooth muscle cells with subsequent dispersion by 6 h, as opposed to specific binding to intracellular smooth muscle components. In contrast to anti-CAT-MAB, anti-SM-MAB showed sustained accumulation within the lesion at 6 h after injection, resulting in a significantly higher %ID/g than in normal portions of aorta (Figs. 6A and B). These results suggest that radiolabeled anti-SM-MAB entering damaged cells in the dissected aorta bound specifically to intracellular smooth muscle myosin without appreciable washout.

For scintigraphic imaging, 74 MBq ^{99m}Tc -anti-SM-MAB (containing approximately 20 μg antibody) were injected into the rats. This amount of radioactive anti-SM-MAB did not, in all rats in the pilot study, sufficiently saturate the smooth muscle myosin antigen exposed in the dissected lesion. In scintigraphic images obtained with ^{99m}Tc -anti-SM-MAB, blood-pool radioactivity tended to mask specific uptake of the lesion at 1 h after injection of the tracer. However, localized activity persisted in the lesion while the blood-pool background activity decreased at 6 h, permitting distinct visualization of the aortic lesion with the gamma camera. These results were confirmed by the quantitative scintigraphic measurement of the uptake ratio. Nonspecific accumulation in the kidneys and in urine in the bladder showed a notable increase at 6 h after injection that could interfere with distinct visualization of the lesion. However, high-quality SPECT images allowed clear stereologic recognition of the lesion irrespective of physiologic urinary tract accumulation.

A previous study showed that murine MAB was quickly and stably labeled with ^{99m}Tc , without loss of antigen-binding activity, by the direct labeling method used in this study (13,14). Labeling efficiency was sufficiently high to permit injection of ^{99m}Tc -labeled anti-SM-MAB without further purification, and the uptake ratio of ^{99m}Tc -anti-SM-MAB at 6 h after injection was sufficiently high to permit SPECT for more distinct visualization of the site and extent of lesions.

Recent progress in vascular biology has yielded markers specific to vascular components. Previously reported characterization of the SM-MHC and its isoforms by us and by other investigators has shown SM-MHC to be a structural protein specific to smooth muscle lineage (17–22). Given that SM-MHC could serve as a specific marker for diseases affecting smooth muscle, a new biochemical method has been developed to diagnose aortic dissection on the basis of immunoassay using an anti-SM-MHC-MAB (4–6). The sensitivity of this immunoassay for detecting aortic dissection is extremely high within the first 24 h after occurrence. However, beyond the first 24 h, smooth muscle myosin rapidly disappears from the circulation, limiting the usefulness of this method. In contrast, as an intracellular structural component, smooth muscle myosin remains in the damaged smooth muscle cells of the dissected aorta and provides a specific target for radioimmunoimaging. From this point of view, we successfully performed immunoscintigraphy using anti-SM-MAB 1 and 2 wk after experimental aortic dissection in rats, confirming specific scintigraphic visualization of the lesions even at 1 wk. Immunoscintigraphy with anti-SM-MAB has potential advantages over the serum assay in detecting aortic dissection in the subacute phase and in displaying the anatomic localization of the lesion. Clinical application of this disease-specific method along with other available diagnostic tools, especially with the immunoassay, may improve diagnostic accuracy and clinical management in cases of aortic dissection.

Despite the encouraging results obtained, two important problems remain to be addressed before clinical application: relatively high blood-pool activity in early images and induction of human antimurine antibodies. Use of Fab fragments rather than intact murine anti-SM-MAB should decrease both blood-pool activity and human antimurine antibody production. However, the successful radioimaging of experimental aortic dissection shown in this study should strongly encourage clinical application of immunoscintigraphy to aortic dissection and spur the necessary further preclinical and clinical investigation.

CONCLUSION

We showed that ^{99m}Tc -labeled anti-SM-MAB specifically accumulated in aortic dissections that were produced experimentally in rats, allowing distinct visualization of the lesion with noninvasive gamma scintigraphy. Radioimmuno-scintigraphy using anti-SM-MAB shows preclinical promise as a noninvasive diagnostic method for imaging aortic dissection.

ACKNOWLEDGMENTS

The authors thank Kiyonori Hatsushiba and Hidenori Otake for valuable technical support with immunoscintigraphic processing. This study was supported by grants-in-aid 08670758 and 09670695 for scientific research from the

REFERENCES

1. McCloy RM, Spittell JA Jr, McGoon DC. The prognosis in aortic dissection (dissecting aortic hematoma or aneurysm). *Circulation*. 1965;31:665-669.
2. Jamieson WRE, Munro AI, Miyagishima RT, Allen P, Tyers GFO, Gerein AN. Aortic dissection: early diagnosis and surgical management are the key to survival. *Can J Surg*. 1982;25:145-149.
3. Nienaber CA, von Kodolitsch Y, Nicolas V, et al. The diagnosis of aortic dissection by noninvasive imaging procedures. *N Engl J Med*. 1993;328:1-9.
4. Katoh H, Suzuki T, Hiroi Y, et al. Diagnosis of aortic dissection by immunoassay for circulating smooth muscle myosin. *Lancet*. 1995;345:191-192.
5. Katoh H, Suzuki T, Yokomori K, et al. A novel immunoassay of smooth muscle myosin heavy chain in serum. *J Immunol Methods*. 1995;185:57-63.
6. Suzuki T, Katoh H, Watanebe M, Kurabayashi M, Yazaki Y, Nagai R. Novel biochemical diagnostic method for aortic dissection: results of a prospective study using an immunoassay of smooth muscle myosin heavy chain. *Circulation*. 1996;93:1244-1249.
7. Khaw BA, Fallon JT, Beller GA, Haber E. Specificity of localization of myosin-specific antibody fragments in experimental myocardial infarction: histologic, histochemical, autoradiographic and scintigraphic studies. *Circulation*. 1979;60:1527-1531.
8. Khaw BA, Gold HK, Yasuda T, et al. Scintigraphic quantification of myocardial necrosis in patients after intravenous injection of myosin-specific antibody. *Circulation*. 1986;74:501-508.
9. Yasuda T, Palacios IF, Dec GW, et al. Indium 111-monoclonal antimyosin antibody imaging in the diagnosis of acute myocarditis. *Circulation*. 1987;76:306-311.
10. Fischman AJ, Rubin RH, Khaw BA, et al. Radionuclide imaging of experimental atherosclerosis with nonspecific polyclonal immunoglobulin G. *J Nucl Med*. 1989;30:1095-1100.
11. Carrió I, Pier PL, Narula J, et al. Noninvasive localization of human atherosclerotic lesion with indium 111-labeled monoclonal Z2D3 antibody specific for proliferating smooth muscle cells. *J Nucl Cardiol*. 1998;5:551-557.
12. Kanda T, McManus JEW, Nagai R, et al. Modification of viral myocarditis in mice by interleukin-6. *Circ Res*. 1996;78:848-856.
13. Baum RP, Hertel A, Lorenz M, Schwarz A, Encke A, Hor G. Technetium-99m-labelled anti-CEA monoclonal antibody for tumor immunoscintigraphy: first clinical results. *Nucl Med Commun*. 1989;10:345-352.
14. Mather SJ, Ellison D. Reduction-mediated technetium-99m labeling of monoclonal antibodies. *J Nucl Med*. 1990;31:692-697.
15. Yukihiro M, Inoue T, Iwasaki T, Tomiyoshi K, Erlandsson K, Endo K. Myocardial infarction in rats: high resolution single-photon emission tomography imaging with pinhole collimator. *Eur J Nucl Med*. 1996;23:896-900.
16. Kobori K, Suzuki K, Yoshida Y, Ooneda G. Light and electron microscopic studies on rat arterial lesions induced by experimental arterial contraction. *Virchows Arch*. 1979;385:29-39.
17. Nagai R, Larson DM, Periasamy M. Characterization of a mammalian smooth muscle myosin heavy chain cDNA clone and its expression in various smooth muscle types. *Proc Natl Acad Sci USA*. 1988;85:1047-1051.
18. Nagai R, Kuro-o M, Babij P, Periasamy M. Identification of two types of smooth muscle myosin heavy chain isoforms by cDNA cloning and immunoblot analysis. *J Biol Chem*. 1989;264:9734-9737.
19. Kuro-o M, Nagai R, Tsuchimochi H, et al. Developmentally regulated expression of vascular smooth muscle myosin heavy chain isoforms. *J Biol Chem*. 1989;264:18272-18275.
20. Aikawa M, Sivam PN, Kuro-o M, et al. Human smooth muscle myosin heavy chain isoforms as molecular markers for vascular development and atherosclerosis. *Circ Res*. 1993;73:1000-1012.
21. Yanagisawa M, Hamada Y, Katsuragawa Y, Imamura M, Mikawa T, Masaki T. Complete primary structure of vertebrate smooth muscle myosin heavy chain deduced from its complementary DNA sequence. *J Mol Biol*. 1987;198:143-157.
22. Miano JM, Cserjesi P, Ligon KL, Periasamy M, Olson EN. Smooth muscle myosin heavy chain exclusively marks the smooth muscle lineage during mouse embryogenesis. *Circ Res*. 1994;75:803-812.